Vegetation Structural Complexity and Biodiversity Across Elevation Gradients in the Great

Smoky Mountains

Running Title: Structure, Biodiversity and Elevation

Jonathan A. Walter[1], Atticus E. L. Stovall[2], Jeff W. Atkins[3]

[1]Department of Environmental Sciences, University of Virginia, Charlottesville, VA

[2]NASA Goddard Space Flight Center, Biospheric Sciences Lab, Greenbelt, MD

[3]Department of Biology, Virginia Commonwealth University, Richmond, VA

Correspondence: Jonathan Walter, Department of Environmental Sciences, University of

Virginia, Charlottesville, VA, USA.

Email: jaw3es@virginia.edu

Abstract

Questions: Elevation, biodiversity, and forest structure are commonly correlated, but their relationships near the positive extremes of biodiversity and elevation are unclear. We asked 1) How does forest structure vary with elevation in a high biodiversity, high topographic complexity region? 2) Does forest structure predict vascular plant biodiversity? 3) Is plant biodiversity more strongly related to elevation or to forest structure?

Location: Great Smoky Mountains National Park, USA

Methods: We used terrestrial LiDAR scanning (TLS) to characterize vegetation structure in 12 forest plots. We combined two new canopy structural complexity metrics with traditional TLS-derived forest structural metrics and vascular plant biodiversity data to investigate correlations among forest structure metrics, biodiversity, and elevation.

Results: Forest structure varied widely across plots spanning the elevational range of GRSM. Our new measures of canopy density (*Depth*) and structural complexity (*σDepth*) were sensitive to structural variations and effectively summarized horizontal and vertical dimensions of structural complexity. Vascular plant biodiversity was negatively correlated with elevation, and more strongly positively correlated with vegetation structure variables.

Conclusions: The strong correlations we observed between canopy structural complexity and biodiversity suggest that structural complexity metrics could be used to assay plant biodiversity over large areas in concert with airborne and spaceborne platforms.

Keywords: LiDAR, structural complexity, species richness, topography

Introduction

Habitat physical structure, biodiversity, and topography are interrelated elements controlling key ecosystem functional properties. Canopy structural complexity—the arrangement of wood and foliar elements in plant canopies—correlates positively with tree biodiversity (Gough et al. 2019) for complex, interrelated reasons. Different tree species may have different growth forms (Verbeeck et al. 2019). More diverse forests, it follows, may have more growth forms represented, and thus have more building blocks with which to construct structural complexity (Gough et al. accepted). A more structurally complex forest tends to have increased available niche space for other flora and fauna species, for example by creating microhabitats (Hansen et al. 1994; Hyde et al. 2006). In mountainous regions, air temperature, solar radiation, and atmospheric pressure all vary as a direct function of elevation (Körner 2007); but state variables such as light availability (i.e. photosynthetically available radiation, or PAR), soil moisture, soil temperature, and nutrient availability covary as a function of elevation and topographic heterogeneity (Alves et al. 2010). These processes are reflected in how elevation influences both plant biodiversity and forest structure. Plant biodiversity tends to decline with increasing elevation (Homeier et al. 2010; Toledo-Garibaldi & Williams-Linera 2014), while canopy height and structural complexity also tends to change with altitude (Homeier et al. 2010). For example, along a 3300 m elevational gradient in South America extending from the Amazon lowlands to the tree line in the Peruvian Andes, changes in forest structure were manifested as decreases in canopy height and increases in canopy gap fraction (Asner et al. 2014). While it is clear that elevation, biodiversity, and forest structure are commonly related, it is unclear how they are interrelated near the positive extremes of both biodiversity and elevation.

3

In the southern Appalachians, complex topography creates steep ecological gradients that drive structural and compositional patterns (Whittaker 1956; Harmon et al. 1984) and produce high levels of biodiversity (Latham & Ricklefs 1993; Gough et al. 2019). Southern Appalachian forests, such as those of Great Smoky Mountains National Park (GRSM), are among the most diverse temperate forests in the world with over 100 woody plant species (Latham & Ricklefs 1993). As such, these forests have long been studied for insights into biodiversity (Whittaker 1956), and related topics including forest productivity (Whittaker 1966; Gough et al. 2019), disturbance (Harmon et al. 1984; Atkins et al. 2020), resource acquisition (Atkins et al. 2018), habitat fragmentation (Ambrose & Bratton 1990), pollution (Mathias & Thomas 2018), and land cover change (Turner et al. 2003). Perhaps surprisingly, then, we are unaware of earlier studies relating biodiversity and forest structure in this high-diversity, topographically complex system.

Advances in remote sensing, specifically light detection and ranging (LiDAR), have enabled mapping of forest structure and complexity with unprecedented precision, at plot-level to regional scales (LaRue et al. 2020). Ecological applications of LiDAR have broadened our understanding of resource acquisition (Stark et al. 2015; Atkins et al. 2018), allocation strategies (Stovall et al. 2017; Stovall et al. 2018b; Stovall & Shugart 2018; Stovall et al. 2018a), use efficiencies (Hardiman et al. 2013), drought response (Atkins & Agee 2019; Smith et al. 2019; Stovall et al. 2019), productivity (Gough et al. 2019), and disturbance history (Fahey et al. 2015; Atkins et al. 2020). However, recent studies of forest structural complexity either focus on broad, landscape to continental scale patterns (LaRue et al. 2018; Atkins et al. 2018; Gough et al. 2019; Fahey et al. 2019), or are limited to characterizations of stand-scale phenomena (Hardiman et al. 2018; Hickey et al. 2019), without fully considering how forest complexity varies at the stand to regional scale in response to ecological gradients.

Forest structure is most commonly characterized using two-dimensional indices that describe either vertical or horizontal space only, often ignoring canopy structural traits that describe internal canopy characteristics (Paynter et al. 2018; Fahey et al. 2019) or how forest structure varies simultaneously along both the vertical and horizontal axes. For instance, horizontal structural heterogeneity can be characterized via passive (optical) remote sensing as variation in canopy cover (Morton et al. 2014; Verrelst et al. 2015), while active (radar and LiDAR) remote sensing captures vertical heterogeneity as changes in canopy height (Camaretta et al. 2019). Both metrics of forest structural complexity focus on the outer canopy and ignore internal canopy characteristics (e.g. canopy structural traits such as layering or foliage density). Internal canopy structure can be inferred using statistically derived metrics such as the 90th percentile or standard deviation of LiDAR measured heights above ground level. Statistical metrics derived directly from LiDAR point clouds can be effective and efficient for predictive models of species biodiversity (Goetz et al. 2007), but lack ecological meaning and may be unstable or non-transferrable across forest types. Recent developments of ecology-based structural metrics that effectively characterize internal canopy structural traits (Atkins et al. 2018; Fahey et al. 2019) describe two-dimensional structure over ground-based transects and are unable to fully capture three-dimensional complexity. Since biodiversity is often dependent on the interior of the forest canopy, new metrics need to be developed that synthesize the canopy structural traits such as layering, density, canopy height, and openness in three-dimensional space.

To understand relationships between forest structure, biodiversity, and elevation in a topographically complex, high-biodiversity region, we used three-dimensional terrestrial lidar scanning (TLS) to sample 12 forest plots in Great Smoky Mountains National Park that were

previously inventoried by the National Ecological Observatory Network (NEON). We developed two new canopy structural complexity metrics and combined them with traditional TLS-derived forest structural metrics and vascular plant biodiversity data to address the following questions: 1) How does forest structure vary with elevation in a high biodiversity, high topographic complexity region? 2) Does forest structure predict vascular plant biodiversity? 3) Is plant biodiversity more strongly related to elevation or to forest structure?

Methods

Study Area and Site Description

Great Smoky Mountains National Park (35.56 N, -83.50 W; denoted as NEON site GRSM) has a humid, continental climate with a mean annual temperature of 13.3 °C. Precipitation is highly variable, with low-elevation valleys receiving on average 1400 m per year, while upper-elevations can receive in excess of 2200 m per year. Elevations in GRSM range from 270 m to 2025 m. The park is over 95% forested, with forests that occupy drier, colder ridges and mountaintops—higher elevations above 1600m—often populated by hemlock (*Tsuga canadenesis*), balsam fir (*Abies balsamea*), fraser fir (*Abies fraseri*), and red spruce (*Picea rubens*) (Narayanaraj et al. 2010; Walter et al. 2017). Sheltered valley regions at lower elevations may have dense cove forests where tuliptree (*Liriodendron tulipifera*), red maple (*acer rubrum*) and oak (*quercus spp.*) abound. Much of the area is covered by thick understories of evergreen shrub, primarily mountain laurel (*Kalmia latifolia*) and rhododendron (*Rhododendron spp.*) (Elliott & Vose 2012). The park is home to over 1,400 flowering plant species and over 4,000 species of non-flowering plants; geologically, GRSM is primarily Precambrian siltstone and sandstone from the Snowbird group.

Data Collection and Post-Processing

Terrestrial LiDAR, or terrestrial laser scanning (TLS), captures detailed 3D information of the forest, enabling the reconstruction and quantitative analysis of forest structure. We visited 12 National Ecological Observatory Network (NEON) distributed vegetation plots (Kao et al. 2012) located in GRSM (Figure 1). Plots were chosen based on field accessibility and ancillary NEON data availability at time of analysis. Four TLS scans were acquired at plot center and three points around center in each of 12 plots between August 23 and 25, 2018 using two Faro Focus 1203D scanners (FARO, Lake Mary, FL, USA). Scans were taken at 1/5 resolution and 4x quality for a total of 28.2 million pulses per scan. All returns with intensity lower than 650 (maximum value = 2100) were removed. Filtering low intensity returns reduces noise and ensures gaps are correctly identified.

Filtered scans were used to estimate the vertical distribution of plant material or plant area vegetation density (PAVD) at the plot-level. We roughly follow the method described by Calders et al. (2014): [i] elevation normalization, [ii] calculate gap probability, [iii] estimate PAVD. The one key difference in the current study is the adoption of a fully 3D digital elevation model to normalize topographic effects, as opposed to simple plane fitting. We found plane fitting was inappropriate in the complex topography of the GRSM national park, resulting in overestimates of total canopy height and a misrepresentation of the vegetation distribution. Topographic normalization followed the following procedure: [i] estimate ground surface, [ii] remove spikes and anomalous points, and [iii] refit and normalize TLS data with 5 m surface model. The ground surface is first estimated as the 1st percentile of height from TLS points in a 5 m grid over a 200 m x 200 m area. The initial model is optimized to remove spikes by excluding all pixels greater than 40% slope. The remaining pixels are refit using a k-nearest

neighbor inverse distance weighting (k = 21) and the resulting surface model is subtracted from the height measurements in the TLS data.

PAVD distributions are derived from a simple calculation of the vertically resolved gap probability (*Pgap*). *Pgap* is calculated as:

$$Pgap(\bar{\theta}, z) = 1 - \frac{\sum (z_i < z, \bar{\theta})}{N(\bar{\theta})}, \tag{1}$$

where z is the height above ground and $\bar{\theta}$ is the midpoint of the 5-degree zenith angle bin used to aggregate the LiDAR returns. The equation essentially calculates the cumulative number of returns per unit height divided by the total number of outgoing laser pulses. In essence, as more vegetation is intercepted, the probability of a laser pulse escaping the canopy decreases.

PAVD is accurately estimated at the hinge angle (a viewing zenith angle of 57.5 degrees) with *Pgap*. The hinge angle is used to estimate total VAI as this is the angle at which the G-Function is nearly invariable at 0.5 for all typical leaf angle distributions (MacArthur & Horn 1969; Jupp et al. 2008). A 5-degree zenith bin between 55 and 60 degrees is used to approximate the hinge angle region. *Pgap* is converted to the cumulative VAI distribution with respect to height aboveground ($L(z)$) using:

$$L(z) \approx -1.1 \log\big(Pgap(57.5)\big). \tag{2}$$

Estimates of $L(z)$ at the top of the canopy approximate the total VAI for a particular sample location. Once cumulative VAI is estimated, *Pgap* is calculated at 5-degree zenith angle bins from 0-60 degrees and weighted by the sine of the zenith angle to sample the uppermost area of the hemisphere viewable by the laser scanner. Finally, the total VAI in each 1 m vertical bin is estimated as the 1st derivative of the $L(z)$ curve after weighting with respect to zenith angle.

Metrics

We derived a suite of structural metrics from TLS data to characterize the horizontal and

vertical distribution of vegetation (Table 1). As described above, we derived the cumulative VAI,

and subsequently, PAVD, for every scan location. Using the PAVD, we calculated foliage

density dependent median height and 80th and 90th percentiles (i.e. the height at which 80% or

90% of foliage falls below). While these metrics summarize vertical structure, they are unable to

quantitatively describe trends in horizontal structure. For this reason, we developed a new metric

we call *Depth*, which describes percentiles of canopy penetration at the hinge angle. *Depth*

percentiles are calculated as the distance from the laser scanner at which a certain percentage of

the total number of returns are observed for 10-degree azimuth bins. A single scan produces 36

estimates of *Depth* from which a standard deviation can be calculated, which we denote *σDepth*.

For this work, we derived mean and standard deviation values from median *Depth* estimates for

each azimuth angle bin; Other percentiles of depth can be calculated (e.g. 80th, 90th), but were

colinear with the median estimates, so we use median as the basis for all subsequent analyses.

The inherent benefit of using *Depth* percentiles and variability is that this information

synthesizes vertical and horizontal structural complexity and allows for normalized comparisons

among scans, regardless of canopy height.

Relationships between biodiversity, elevation, and forest structure

We used NEON vascular plant diversity data from 12 NEON plots coinciding with our

TLS scans. Plant abundance of each 400 m^2 (20 m x 20 m) plot was sampled using a nested

hierarchical protocol in which presence was observed in eight 1 m^2 subplots and eight 10 m^2

subplots distributed within four 100 m^2 subplots. Subplots were aggregated to plot level. We used plant abundance data from July and August 2017. We quantified plot biodiversity using species richness. Diversity indices that take into account abundance, such as Shannon's Index and Simpson's Index, were deemed inappropriate given the orders-of-magnitude sizes differences in the species included in NEON's dataset (all vascular plants, including trees).

Pearson correlation was used to quantify how plant species richness is correlated with elevation and TLS-derived forest structural metrics. We considered the forest structural metrics vegetation-area index (VAI), canopy height (90th percentile of TLS returns), *Depth*, and *σDepth*. To obtain forest structural metrics at the plot level, we averaged metrics for all scans taken at each plot (*n* = 3 to 5). Statistical analyses were conducted in R 3.6.2 (R Core Team 2020).

Results

Forest Structure and Complexity

Forest structure varied widely across plots spanning the elevational range of GRSM. Canopy height ranged from ca. 10 to 35 m (Figure 3). Canopies between 15 and 25 m had the highest variability in PAVD distributions, showing that vegetation layering differs among and within plots (Figure 3). The high elevation locations were dominated by dense conifers with a notable presence of coarse woody debris (e.g. large, downed trees) and standing dead, while the taller locations in lower elevations were more open throughout the canopy (Table 2).

Our measures of canopy density (*Depth*) and structural complexity (*σDepth*) were sensitive to structural variations and effectively summarized variability in canopy structure in the horizontal and vertical dimensions (Figure 4). *Depth* summarized information about the density and height of the canopy. Plots with similar *Depth* could have substantially different *σDepth*, as

this metric captures how variable *Depth* is across all 10-degree azimuth bins. Higher $\sigma Depth$ is indicative of canopies with high variability in vegetation structure: high density vegetation and gaps distributed throughout the canopy.

Forest structural metrics considered in this study were moderately to strongly correlated with each other (Figure 5). Lower stature canopies had higher VAI in GRSM (Figure 4). VAI was also moderately negatively correlated with both *Depth* and $\sigma Depth$, but taller canopies were consistently more structurally complex (Figure 5). Total VAI was of less relative importance than canopy height in capturing changes in structural variability (Figure 5). *Depth* and $\sigma Depth$ were strongly positively correlated with each other (Figure 5).

Topographic gradients in the GRSM controlled forest structure and complexity (Figure 6). Canopy height declined with increasing elevation. VAI was highest in the high-elevation plots, and lowest in the low elevation plots. Forest complexity, as measured by *Depth* and $\sigma Depth$ decreased from low to high elevation.

Biodiversity

Plant species richness varied widely among plots, from 4 to 47 species (Table 2). Species richness was not significantly correlated with VAI (Figure 7; Pearson $r = -0.39$, $p = 0.205$, but was strongly positively correlated with canopy height ($r = 0.80$, $p = 0.002$), *Depth* ($r = 0.77$, $p = 0.004$), and $\sigma Depth$ ($r = 0.84$, $p < 0.001$). Plant species richness was also negatively correlated with elevation ($r = -0.66$, $p = 0.018$). The correlations between biodiversity and forest structural metrics were stronger than the correlation between biodiversity and elevation (Figure 7). Although the strongest correlate of plant species richness was $\sigma Depth$, the confidence interval on r included the estimates for canopy height and *Depth*.

Discussion

In this study, we developed two new forest structural complexity metrics suited to quantifying aspects of the 3D structure of forests (*Depth* and σ*Depth*) and investigated how they correlate with elevation and biodiversity across a high-biodiversity, high-relief area in Great Smoky Mountains National Park. Statistically derived LiDAR structural metrics have been limited by either focusing solely on characterizing either horizontal structure (Fischer et al. 2019) or vertical structure (Fotis et al. 2018; Kamoske et al. 2019), or by a lack of true representation of how 3D structure varies with space (Stark et al. 2015; Atkins et al. 2018; Hardiman et al. 2018). Capturing the complex relationships between biodiversity and physical structure requires the summation of multiple dimensions of variability, including the biological and physical. The bounds of forest structural complexity are likely set by the species pool from which that forest draws. *Depth* and σ*Depth* metrics likely correlate strongly with measures of species richness since the greater the number of species, the more likely the species included will be architecturally dissimilar from others. These metrics capture canopy structural traits such as vegetation density and complexity, summarized in both vertical and horizontal dimensions. In doing so, these metrics describe the internal arrangement of the forest, characterizing where space is being filled by foliar elements.

Across the high-biodiversity, high-relief and topographically complex Great Smoky Mountains, both forest structural complexity and vascular plant biodiversity tended to decline with elevation. One goal of this study was to examine whether elevation-biodiversity-complexity relationships persist in a regional biodiversity hotspot. In this case, we observed high among-plot variability in plot-level species richness (alpha-diversity), even as high regional species richness (gamma-diversity) was maintained by substantial species turnover among plots (beta-diversity).

The elevational gradient in GRSM seems to create a microcosm of latitudinal clines in biodiversity, where an increasingly inhospitable environment supports fewer species and constrains plant growth (Whittaker 1956; Hawkins et al. 2003; Gillman et al. 2015). However, inference here is limited, the main caveat being an approximately 1000 m gap in elevation between our low and high elevation plots. While many studies of elevation and diversity relationships show monotonic declines in species richness with elevation, there are as many studies showing a humped relationship, with species richness peaking at mid-elevations (Rahbek 1995; Grytnes & Vetaas 2002). It is important to note that "mid-elevation" is relative to the study system—different ranges for what mid-elevation is would exist when comparing the Appalachians to the Rockies, or either to the Himalayas.

It is unclear, despite plant biodiversity being more strongly correlated with forest structure than with elevation, whether structural complexity begets biodiversity, or vice-versa. Indeed, neither direction of causality strictly excludes the other. Structural complexity could enhance biodiversity by creating niche space that can be filled by other species, or biodiversity could enhance structural complexity due to architectural diversity among species creating more ways to build complexity (Gough et al. 2019; Verbeeck et al. 2019) at higher values of species richness. It may, in principle, be possible to disentangle these effects if a scenario with many plots featuring different subsets of an overlapping species pool. However, with a modest number of plots with high beta-diversity, this is not possible in our study.

The strong correlations we observed between canopy structural complexity and biodiversity suggest that structural complexity metrics could be used to assay plant biodiversity over large areas. The availability of LiDAR from airborne platforms is increasing due to programs such as NEON (Kao et al. 2012), and new satellite-borne sensors such as GEDI

13

(Dubayah et al. 2020) create opportunities for quantifying forest structural complexity at fine spatial resolutions over unprecedented geographic extents. Studies such as ours are important precursors, however, because they explicitly link biodiversity and forest structural complexity, but studies in other systems are needed to parameterize the forest structure-biodiversity relationship. The metric foliage height diversity (Tang et al. 2019; Burns et al. 2020), which is an established GEDI data product, captures similar canopy properties to our *Depth* and *σDepth* metrics and is a likely candidate for inclusion in successful predictions of biodiversity from airborne and satellite-borne LiDAR sensors.

Acknowledgements

Author Contributions

The authors contributed equally to the manuscript; author order was determined by the order in which the first letter of their last name appears in the first letter of the words to "King Harvest" by The Band. All authors collected TLS scans; AELS and JWA processed TLS data; AELS developed new TLS metrics; JAW analyzed biodiversity-complexity-elevation relationships. All authors wrote and edited the manuscript.

Data Availability

Data from this study are available on Zenodo. The DOI is: 10.5281/zenodo.3742194.

References

Alves, L.F., Vieira, S.A., Scaranello, M.A., Camargo, P.B., Santos, F.A.M., Joly, C.A., & Martinelli, L.A. 2010. Forest structure and live aboveground biomass variation along and elevational gradient of tropical Atlantic moist forest (Brazil). *Forest Ecology and Management* 260: 679–691.

Ambrose, J.P., & Bratton, S.P. 1990. Trends in Landscape Heterogeneity Along the Borders of Great Smoky Mountains National Park. *Conservation Biology* 4: 135–143.

Asner, G.P., Anderson, C.B., Martin, R.E., Knapp, D.E., Tupayachi, R., Sinca, F., & Malhi, Y. 2014. Landscape-scale changes in forest structure and functional traits along an Andes-to-Amazon elevation gradient. *Biogeosciences* 11: 843–856.

Atkins, J.W., & Agee, E. 2019. Phenological and structural linkages to seasonality inform productivity relationships in the Amazon Rainforest. *New Phytologist* 222: 1165–1166.

Atkins, J.W., Bond-Lamberty, B., Fahey, R.T., Hardiman, B.S., Haber, L., Stuart-Haentjens, E., LaRue, E.A., McNeil, B.E., Orwig, D.A., Stovall, A.E., Tallant, J.M., Walter, J.A., & Gough, C.M. 2020. Multidimensional structural characterization is required to detect and differentiate among moderate disturbance agents. *Ecosphere*

Atkins, J.W., Fahey, R.T., Hardiman, B.H., & Gough, C.M. 2018. Forest Canopy Structural Complexity and Light Absorption Relationships at the Subcontinental Scale. *Journal of Geophysical Research: Biogeosciences* 123: 1387–1405.

Burns, P., Clark, M., Salas, L., Hancock, S., Leland, D., Jantz, P., Dubayah, R., & Goetz, S. 2020. Incorporating canopy structure from simulated GEDI lidar into bird species distribution models. *Environmental Research Letters*. doi: 10.1088/1748-9326/ab80ee

Calders, K., Armston, J., Newnham, G., Herold, M., & Goodwin, N.R. 2014. Implications of sensor configuration and topography on vertical plant profiles deriverd from terrestrial LiDAR. *Agricultural and Forest Meteorology* 194: 104–117.

Camaretta, N., Harrison, P.A., Bailey, T., Potts, B., Lucieer, A., Davidson, N., & Hunt, M. 2019. Monitoring forest structure to guide adaptive management of forest restoration: a review of remote sensing approaches. *New Forests*. doi: 10.1007/s11056-019-09754-5

Dubayah, R., Blair, J.B., Goetz, S., Fatoyinbo, L., Hansen, M., Healey, S., Hofton, M., Hurtt, G., Kellner, J., Luthcke, S., Armston, J., Tang, H., Duncanson, L., Hancock, S., Jantz, P., Marselis, S., Patterson, P.L., Qi, W., & Silva, C. 2020. The Global Ecosystem Dynamics Investigation: High-resolution laser ranging of the Earth's forests and topography. *Science of Remote Sensing* 1: 100002.

Elliott, K.J., & Vose, J.M. 2012. Age and distribution of an evergreen clonal shrub in the Coweeta Basin: Rhododendron maximum L. [1]. *The Journal of the Torrey Botanical Society* 139: 149–166.

Fahey, R.T., Atkins, J.W., Gough, C.M., Hardiman, B.S., Nave, L.E., Tallant, J.M., Nadehoffer, K.J., Vogel, C., Scheuermann, C.M., Stuart-Haëntjens, E., Haber, L.T., Fotis, A.T.,

Ricart, R., & Curtis, P.S. 2019. Defining a spectrum of integrative trait-based vegetation canopy structural types (J. Penuelas, Ed.). *Ecology Letters* 22: 2049–2059.

Fahey, R.T., Fotis, A.T., & Woods, K.D. 2015. Quantifying canopy complexity and effects on productivity and resilience in late-successional hemlock–hardwood forests. *Ecological Applications* 25: 834–847.

Fischer, R., Knapp, N., Bohn, F., Shugart, H.H., & Huth, A. 2019. The Relevance of Forest Structure for Biomass and Productivity in Temperate Forests: New Perspectives for Remote Sensing. *Surveys in Geophysics* 40: 709–734.

Fotis, A.T., Morin, T.H., Fahey, R.T., Hardiman, B.S., Bohrer, G., & Curtis, P.S. 2018. Forest structure in space and time: Biotic and abiotic determinants of canopy complexity and their effects on net primary productivity. *Agricultural and Forest Meteorology* 250: 181–191.

Gillman, L.N., Wright, S.D., Cusens, J., McBride, P.D., Malhi, Y., & Whittaker, R.J. 2015. Latitude, productivity and species richness: Latitude and productivity. *Global Ecology and Biogeography* 24: 107–117.

Goetz, S., Steinberg, D., Dubayah, R., & Blair, B. 2007. Laser remote sensing of canopy habitat heterogeneity as a predictor of bird species richness in an eastern temperate forest, USA. *Remote Sensing of Environment* 108: 254–263.

Gough, C.M., Atkins, J.W., Fahey, R.T., & Hardiman, B.S. 2019. High rates of primary production in structurally complex forests. *Ecology* 100: e02864.

Gough, C.M., Atkins, J.W., Fahey, R.T., Hardiman, B.S., & LaRue, E.A. accepted. Community and structural constraints on the complexity of eastern North American forests. *Global Ecology and Biogeography*

Grytnes, J.A., & Vetaas, O.R. 2002. Species Richness and Altitude: A Comparison between Null Models and Interpolated Plant Species Richness along the Himalayan Altitudinal Gradient, Nepal. *The American Naturalist* 159: 294–304.

Hansen, A.J., Vega, R.M., McKee, A.W., & Moldenke, A. 1994. Ecological processes linking forest structure and avian diversity in western Oregon. In *Biodiversity, Temperate Ecosystems, and Global Change*, pp. 217–245. Springer, Berlind.

Hardiman, B.S., Gough, C.M., Halperin, A., Hofmeister, K.L., Nave, L.E., Bohrer, G., & Curtis, P.S. 2013. Maintaining high rates of carbon storage in old forests: A mechanism linking canopy structure to forest function. *Forest Ecology and Management* 298: 111–119.

Hardiman, B., LaRue, E., Atkins, J., Fahey, R., Wagner, F., & Gough, C. 2018. Spatial Variation in Canopy Structure across Forest Landscapes. *Forests* 9: 474.

Harmon, M.E., Bratton, S.P., & White, P.S. 1984. Disturbance and vegetation response in relation to envlronmental gradients in the Great Smoky Mountains. *Vegetatio* 55: 129–139.

Hawkins, B.A., Field, R., Cornell, H.V., Currie, D.J., Guégan, J.-F., Kaufman, D.M., Kerr, J.T., Mittelbach, G.G., Oberdorff, T., O'Brien, E.M., Porter, E.E., & Turner, J.R.G. 2003. Energy, water, and broad-scale geographic patterns of species richness. *Ecology* 84: 3105–3117.

Hickey, L.J., Atkins, J., Fahey, R.T., Kreider, M.T., Wales, S.B., & Gough, C.M. 2019. Contrasting Development of Canopy Structure and Primary Production in Planted and Naturally Regenerated Red Pine Forests. *Forests* 10: 566.

Homeier, J., Breckle, S.W., Günter, S., & Rollenbeck, R. 2010. Tree diversity, forest structure and productivity along altitudinal and topographical gradients in a species-rich Ecuadorian montaine rain forest. *Biotropica* 42: 140–148.

Hyde, P., Dubayah, R., Walker, W., Blair, J.B., Hofton, M., & Hunsaker, C. 2006. Mapping forest structure for wildlife habitat analysis using multe-sensor (LiDAR, SAR/InSAR, ETM+, Quickbird) synergy. *Remote Sensing of Environment* 102: 63–67.

Jupp, D.L.B., Culvenor, D.S., Lovell, J.L., Newnham, G.J., Strahler, A.H., & Woodcock, C.E. 2008. Estimating forest LAI profiles and structural parameters using a ground-based laser called 'Echidna(R). *Tree Physiology* 29: 171–181.

Kamoske, A.G., Dahlin, K.M., Stark, S.C., & Serbin, S.P. 2019. Leaf area density from airborne LiDAR: Comparing sensors and resolutions in a temperate broadleaf forest ecosystem. *Forest Ecology and Management* 433: 364–375.

Kao, R.H., Gibson, C.M., Gallery, R.E., Meier, C.L., Barnett, D.T., Docherty, K.M., Blevins, K.K., Travers, P.D., Azuaje, E., Springer, Y.P., Thibault, K.M., McKenzie, V.J., Keller, M., Alves, L.F., Hinckley, E.-L.S., Parnell, J., & Schimel, D. 2012. NEON terrestrial field observations: designing continental-scale, standardized sampling. *Ecosphere* 3: art115.

Körner, C. 2007. The use of "altitude" in ecological research. *Trends in Ecology & Evolution* 22: 569–574.

LaRue, E.A., Atkins, J.W., Dahlin, K.M., Fahey, R.T., Fei, S., Gough, C.M., & Hardiman, B.S. 2018. Linking Landsat to terrestrial LiDAR: Vegetation metrics of forest greenness are correlated with canopy structural complexity. *International Journal of Applied Earth Observation and Geoinformation* 73: 420–427.

LaRue, E.A., Wagner, F.W., Fei, S., Atkins, J.W., Fahey, R.T., Gough, C.M., & Hardiman, B.S. 2020. Compatibility of aerial and terrestrial LiDAR for quantifying forest structural diversity. *Preprints*

Latham, R.E., & Ricklefs, R.E. 1993. Global patterns of tree species richness in moist forests: energy diversity theory does not account for variation in species richness. *Oikos* 67: 325–333.

MacArthur, R.H., & Horn, H.S. 1969. Foliage Profile by Vertical Measurements. *Ecology* 50: 802–804.

Mathias, J.M., & Thomas, R.B. 2018. Disentangling the effects of acidic air pollution, atmospheric CO_2, and climate change on recent growth of red spruce trees in the Central Appalachian Mountains. *Global Change Biology* 24: 3938–3953.

Morton, D.C., Nagol, J., Carabajal, C.C., Rosette, J., Palace, M., Cook, B.D., & North, P.R. 2014. Amazon forests maintain consistent canopy structure and greenness during teh dry season. *Nature* 506: 221–224.

Paynter, I., Genest, D., Saenz, E., Peri, F., Boucher, P., Li, Z., Strahler, A., & Schaaf, C. 2018. Classifying ecosystems with metaproperties from terrestial laser scanning data. *Methods in Ecology and Evolution* 9: 210–222.

Rahbek, C. 1995. The elevational gradient of species richness: a uniform pattern? *Ecography* 18: 200–205.

Smith, M.N., Stark, S.C., Taylor, T.C., Ferreira, M.L., Oliveira, E., Restrepo-Coupe, N., Chen, S., Woodcock, T., Santos, D.B., Alves, L.F., Figueira, M., Camargo, P.B., Oliveira, R.C., Aragão, L.E.O.C., Falk, D.A., McMahon, S.M., Huxman, T.E., & Saleska, S.R. 2019. Seasonal and drought-related changes in leaf area profiles depend on height and light environment in an Amazon forest. *New Phytologist* 222: 1284–1297.

Stark, S.C., Enquist, B.J., Saleska, S.R., Leitold, V., Schietti, J., Longo, M., Alves, L.F., Camargo, P.B., & Oliveira, R.C. 2015. Linking canopy leaf area and light enviroment with tree size distributions to explain Amazon forest demography. *Ecology Letters* 18: 636–645.

Stovall, A.E.L., Anderson-Teixeira, K.J., & Shugart, H.H. 2018a. Assessing terrestrial laser scanning for developing non-destructive biomass allometry. *Forest Ecology and Management* 427: 217–229.

Stovall, A.E.L., Anderson-Teixeira, K.J., & Shugart, H.H. 2018b. Terrestrial LiDAR-derived non-destructive woody biomass estimates for 10 hardwood species in Virginia. *Data in Brief*. doi: 10.1016/j.dib.2018.06.046

Stovall, A.E.L., & Shugart, H.H. 2018. Improved biomass calibration and validation with terrestrial LiDAR: Implications for future LiDAR and SAR missions. *IEEE Journal of Selected Topics in Applied Earth Observations and Remote Sensing* 11: 3527–3537.

Stovall, A.E.L., Shugart, H., & Yang, X. 2019. Tree height explains mortality risk during an intense drought. *Nature Communications* 10: 4385.

Stovall, A.E.L., Vorster, A.G., Anderson, R.S., Evangelista, P.H., & Shugart, H.H. 2017. Non-destructive aboveground biomass estimation of coniferous trees using terrestrial LiDAR. *Remote Sensing of Environment* 200: 31–42.

Tang, H., Armston, J., Hancock, S., Marselis, S., Goetz, S., & Dubayah, R. 2019. Characterizing global forest canopy cover distribution using spaceborne lidar. *Remote Sensing of Environment* 231: 111262.

Toledo-Garibaldi, M., & Williams-Linera, G. 2014. Tree diversity patterns in successive vegetation types along an elevation gradient in the mountains of eastern Mexico. *Ecological Research* 29: 1097–1104.

Turner, M.G., Pearson, S.M., Bolstad, P., & Wear, D. 2003. Effects of land-cover change on spatial pattern of forest communities in the Southern Appalachian Mountains (USA). *Landscape Ecology* 18: 449–464.

Verbeeck, H., Bauters, M., Jackson, T., Shenkin, A., Disney, M., & Calders, K. 2019. Time for a Plant Structural Economics Spectrum. *Frontiers in Forests and Global Change* 2: 43.

Verrelst, J., Camps-Valls, G., Muñoz-Marí, J., Rivera, J.P., Veroustraete, F., Clevers, J.G., & Moreno, J. 2015. Optical remote sensing and the retrieval of terrestrial bio-geophysical properties--A review. *ISPRS Journal of Photogrammetry and Remote Sensing* 108: 273–290.

Whittaker, R.H. 1966. Forest dimensions and production in the Great Smoky Mountains. *Ecology* 47: 103–121.

Whittaker, R.H. 1956. Vegetation of the great smoky mountains. *Ecological Monographs* 26: 1–80.

Tables

Table 1. Definitions of terrestrial lidar derived structural terms.

Metric	Definition	Source
Vegetation Area Index (VAI)	One-sided area of all vegetation elements, including leaf, branches, etc.	MacArthur and Horn 1969; Jupp et al. 2008; Atkins et al. 2018
Height Percentiles (e.g. p10, p90)	Percentile height of foliage distribution or Plant Area Vegetation Density (PAVD; e.g. p90 is the height at which 90% of the vegetation is below).	Lefsky et al. 2003;
Depth	Percentile of distance or depth specifically at 57.5° zenith angle (e.g. d95 is the distance at which 95% of all lidar returns have occurred).	This paper
σDepth	The standard deviation of all mean depth measurements at the 57.5° zenith angle in 10 degree azimuth bins.	This paper

Table 2: Plot elevation, biodiversity, and forest structural metrics. Plot IDs correspond to NEON plot designations. The p90 metric corresponds to canopy height.

Plot ID	Elevation	Richness	VAI	p90	*Depth*	*σDepth*
GRSM_001	467 m	41	3.59	27.25 m	11.00 m	6.51 m
GRSM_002	969 m	9	3.50	20.67 m	6.32 m	2.97 m
GRSM_006	527 m	22	3.96	19.25 m	6.56 m	3.65 m
GRSM_013	561 m	31	3.88	19.75 m	5.76 m	3.66 m
GRSM_014	545 m	34	3.59	29.75 m	10.33 m	5.48 m
GRSM_016	1778 m	7	4.02	15.50 m	4.51 m	2.76 m
GRSM_020	608 m	44	4.02	23.75 m	7.14 m	4.19 m
GRSM_021	587 m	47	3.25	30.33 m	11.03 m	6.37 m
GRSM_024	624 m	11	3.54	17.75 m	3.53 m	2.99 m
GRSM_025	1791 m	9	4.52	11.33 m	3.34 m	1.27 m
GRSM_027	1973 m	17	3.59	10.00 m	2.43 m	1.18 m
GRSM_029	1786 m	4	4.02	15.00 m	5.75 m	2.04 m

Figures
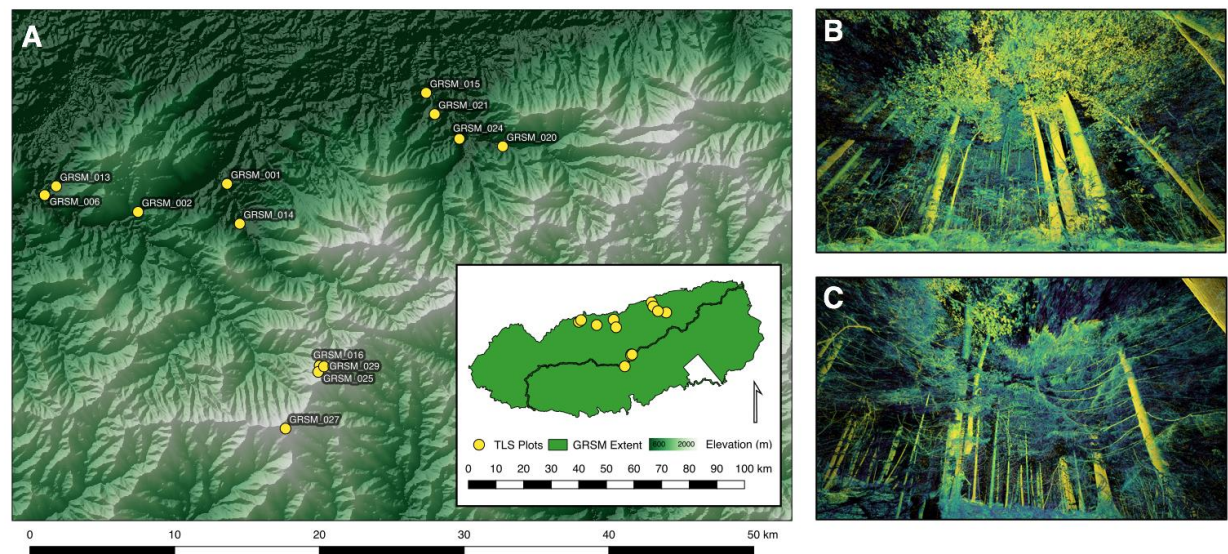
Figure 1: Overview [A] the Great Smokey Mountains National Park study area and examples of terrestrial laser scanning data in [B] low-elevation broadleaf and [C] high-elevation conifer plots.
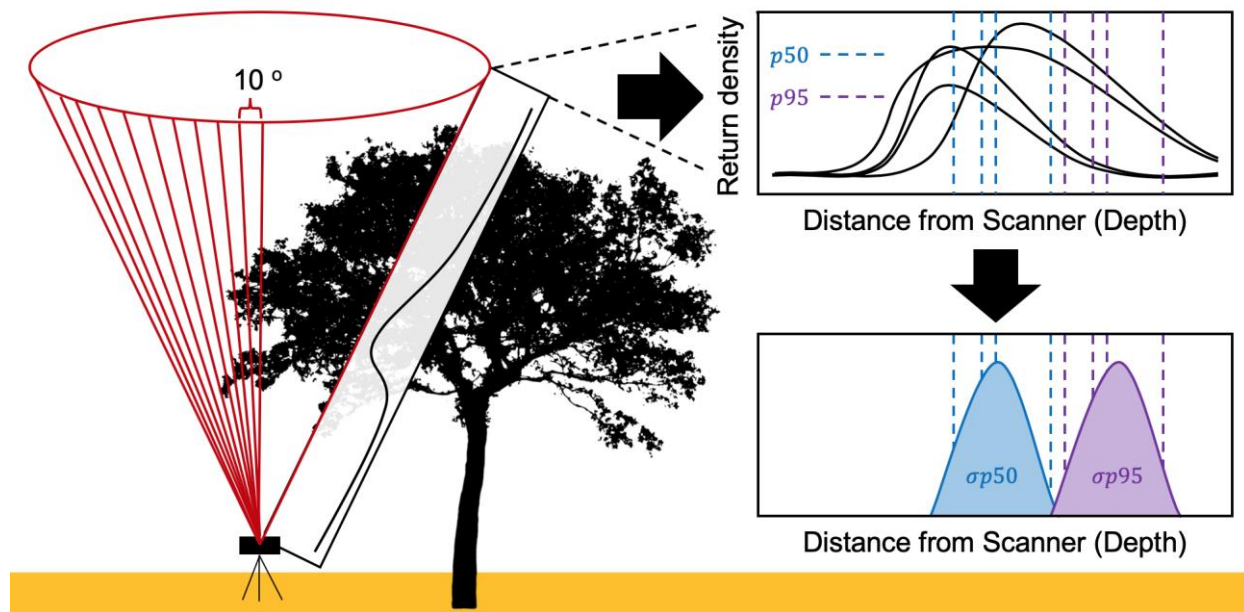
Figure 2: Method of deriving σDepth complexity metric from TLS scans. For each 10-degree

azimuthal bin, the distribution of return density with respect to distance from the scanner is

calculated. Next, the median (p50) is calculated, along with any other necessary percentiles (e.g.

p95). The standard deviation of all depth percentiles in individual 10-degree azimuthal bins

(σDepth) provides an estimate of structural complexity.
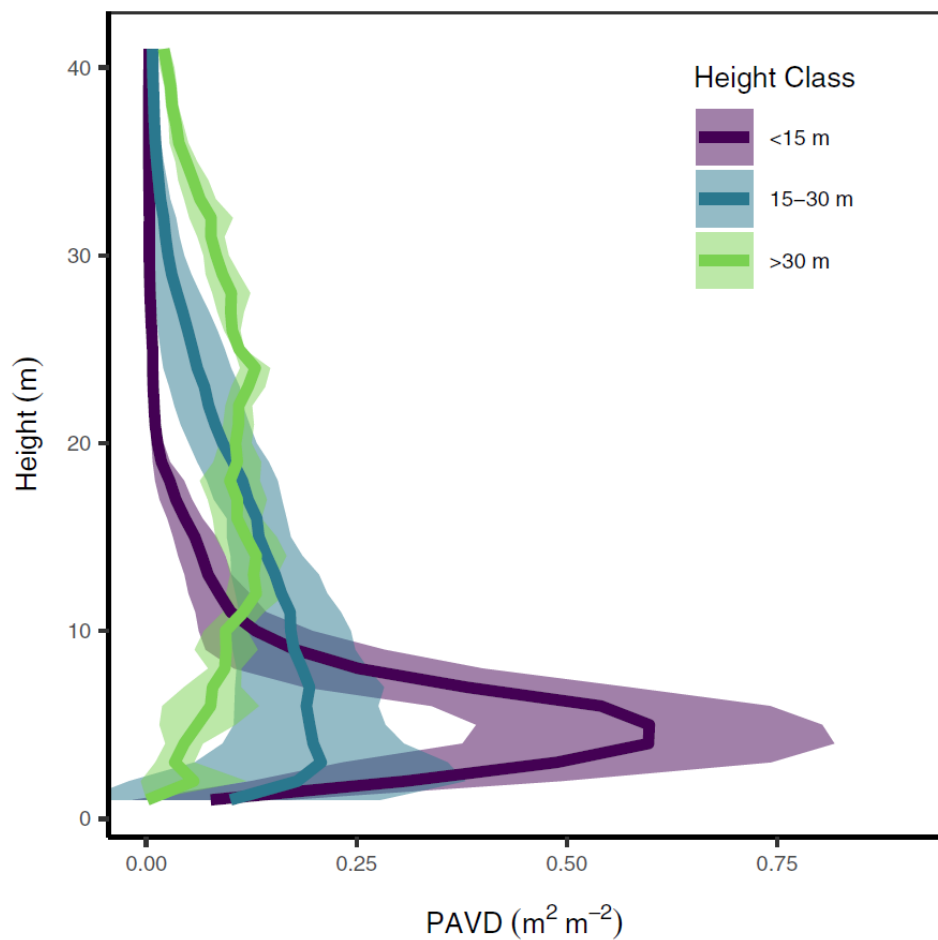
Figure 3: PAVD distributions for 3 canopy height classes. Low stature (<15 m) canopies exhibited dense foliage, while medium (15-30 m) and large (>30 m) canopies had more evenly distributed foliage.
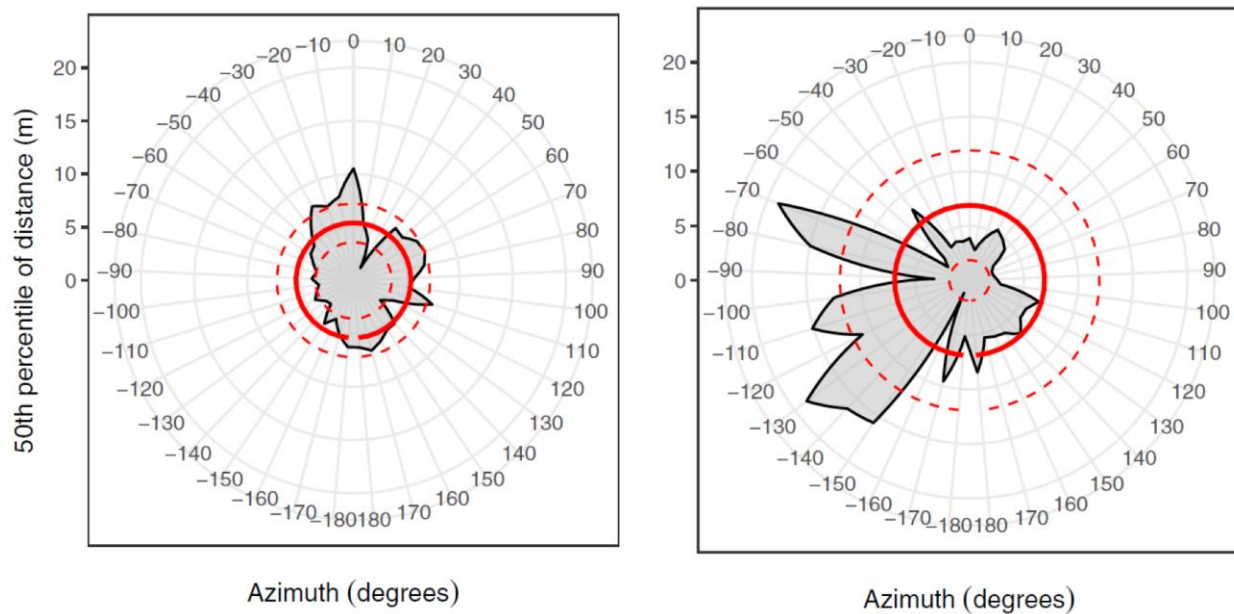
Figure 4: Visualization of plots with different internal canopy complexity: (left) dense vegetation with few gaps (plot = GRSM_029; depth = 5.4 m; sd(depth)=1.8 m) and (right) open canopy with high complexity (plot = GRSM_013, depth = 6.9 m; sd(depth)=5.0 m). We derive the openness and complexity metric at the 57.5 view angle. The black line is the 50th percentile (median) distance from the scanner in each 10-degree azimuth bin. The mean (Depth; solid red line) and ± one standard deviation (σDepth; dashed red lines) of azimuth-binned 50th percentile distances are the basis for our new structural complexity metrics.
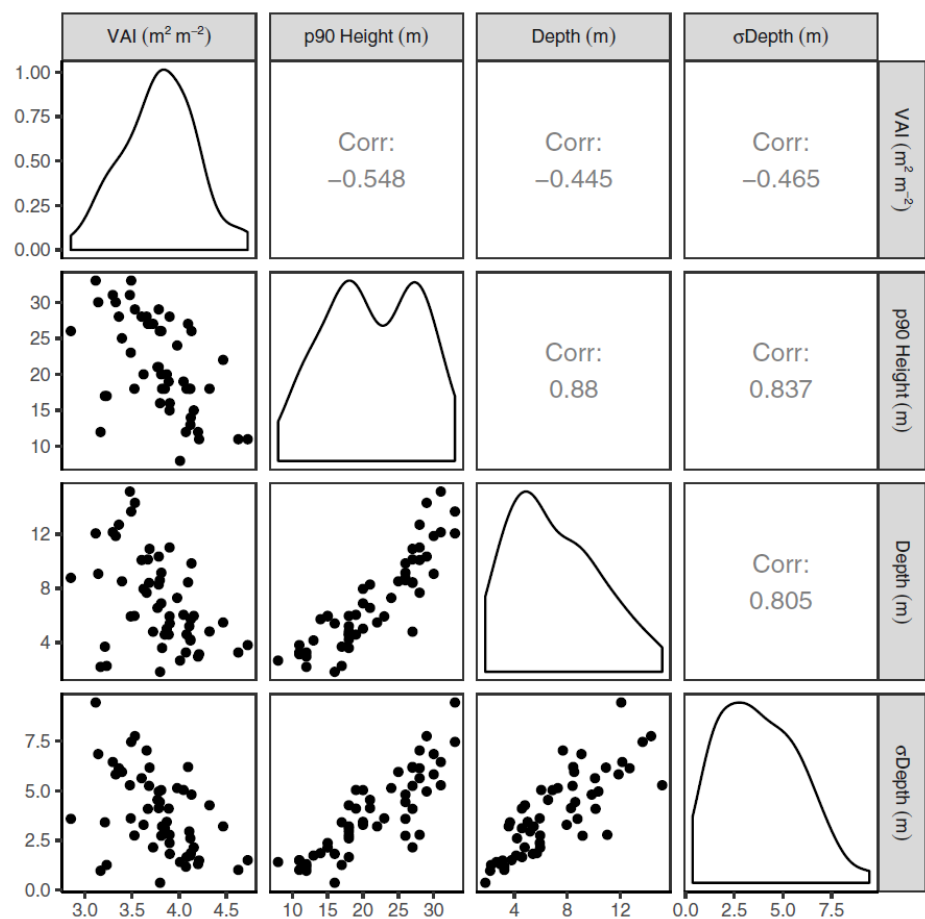
Figure 5. Distributions of and correlations between forest structural metrics for individual TLS scans. Correlation is measured using Pearson correlation.
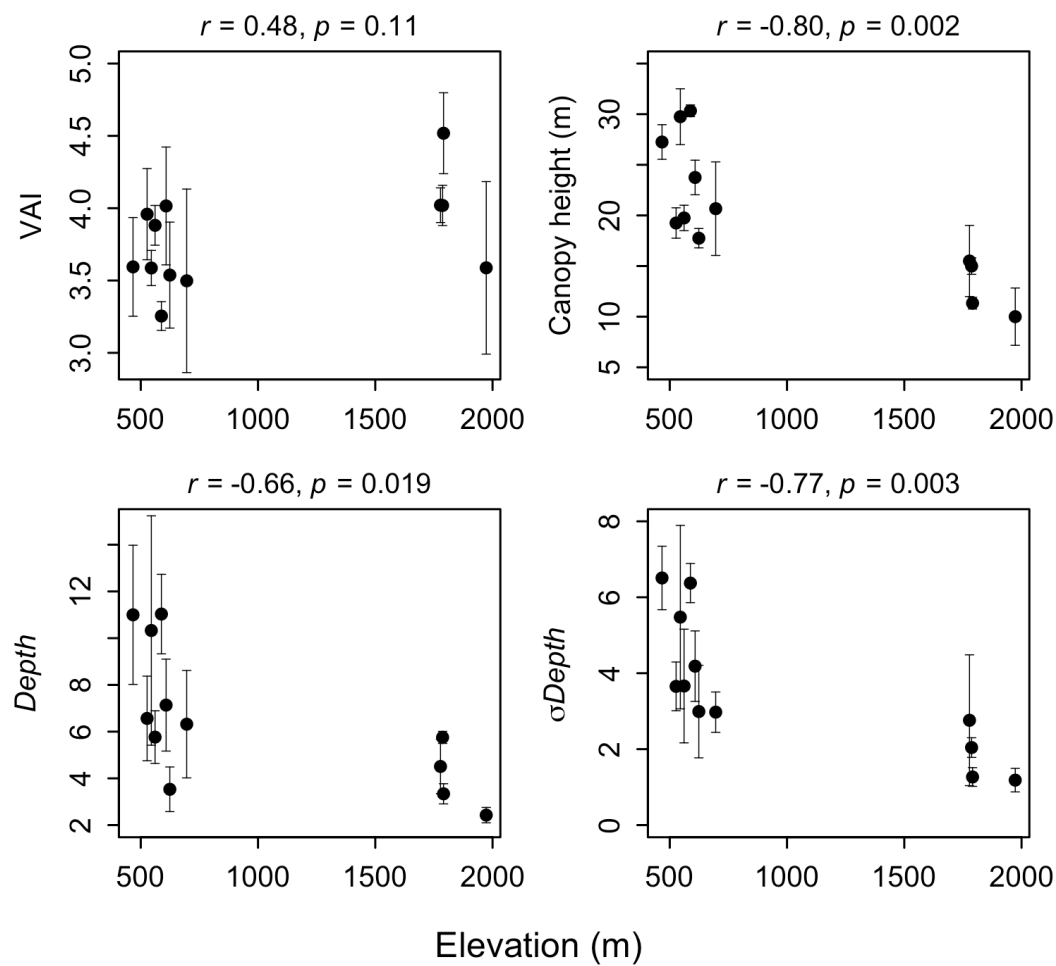
Figure 6. Correlations between forest structural metrics and elevation. Correlation (*r*) is measured using Pearson correlation, and nominal *p*-values assume independent tests.
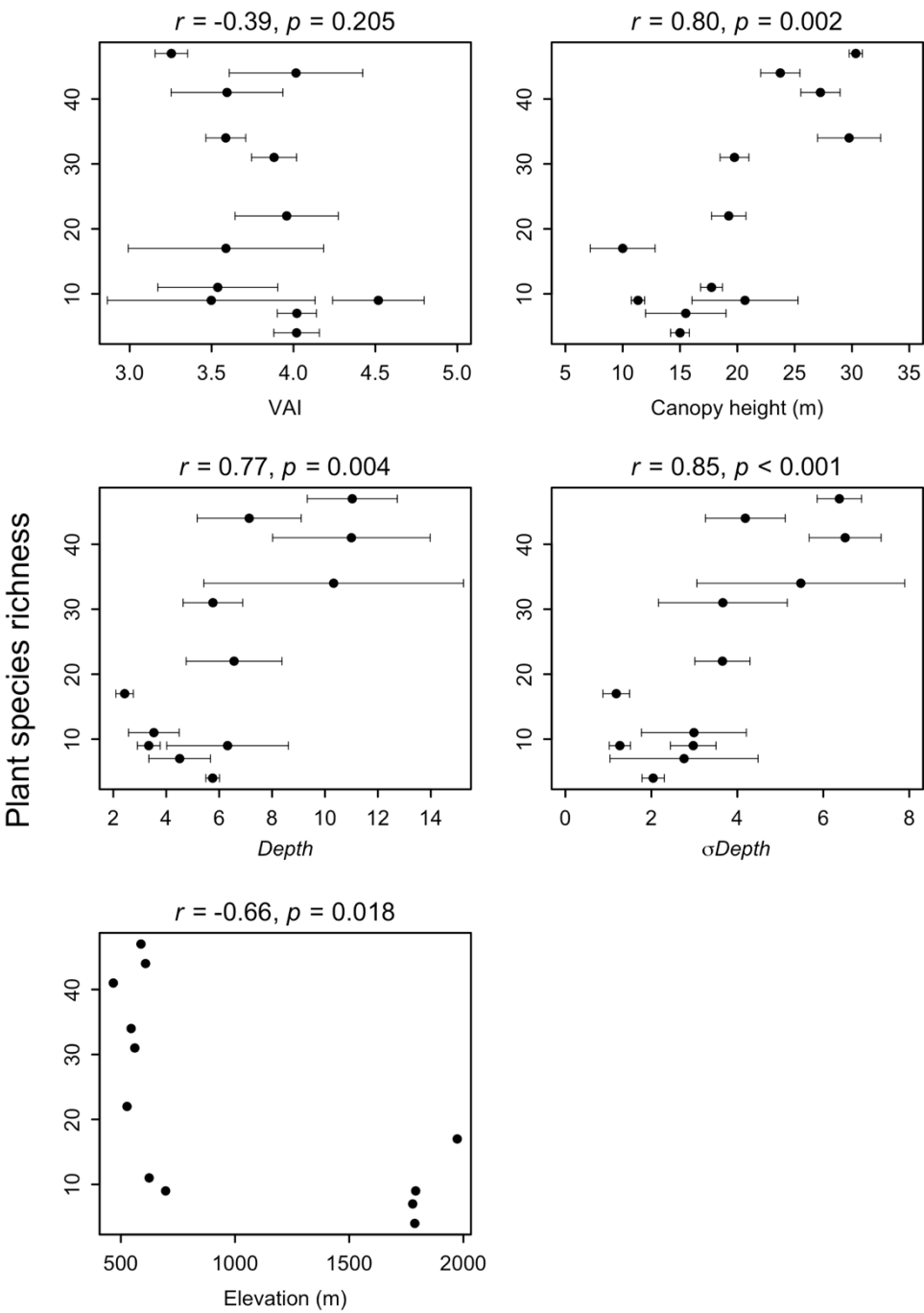
Figure 7. Plant species richness is correlated with structural complexity metrics and elevation.

Correlation (*r*) is measured using Pearson correlation, and nominal *p*-values assume independent

tests.